Chapter 11
Surface Roughness Scattering in MOS Structures

Raheel Shah and Merlyne DeSouza

Abstract The comprehensive Ando's surface roughness (SR) model examined for nMOSFETs. Four distinct source terms contribute in SR scattering. Relative strength of these contributing source terms are evaluated and compared. The most influential term turned out to be due to scattering with the "physical steps" at the interface. Remote SR scattering is also significant in ultra-thin MOS structures. The proposed model of Gámiz et al. for remote SR scattering is studied. It is shown that modification to the Gámiz model is necessary in order to observe the full impact of rms height of the abrupt "steps".

Keywords Surface roughness · ultra-thin MOSFET · mobility · modelling and simulations

11.1 Introduction

Apart from electron-phonon scattering the most damaging effect to charge carrier mobility in MOS structures is scattering at the rough insulator/substrate interface. This scattering is particularly dominant at high inversion densities, however, due to its nature, it weakly depends on lattice temperature variations. Unlike phonon scattering it is not intrinsic in nature, since with technological advancement the insulator can be grown on the substrate with relative smoothness.

Theoretical models of interface scattering date back to 1968, when Prang and Nee performed simulations to quantify the irregularities of a rough surface [1]. This was followed by a model with explicit mobility dependence on the transverse effective

R. Shah (✉)
Emerging Technologies Research Centre, De Montfort University LE1 9BH, UK
e-mail: raheel@dmu.ac.uk

M. DeSouza
EEE Department, University of Sheffield, Mappin Street, Sheffield S1 3JD, UK
e-mail: m.desouza@sheffield.ac.uk

S.-I. Ao and L. Gelman (eds.), *Electronic Engineering and Computing Technology*, Lecture Notes in Electrical Engineering 60, DOI 10.1007/978-90-481-8776-8_11,

field by Matsumoto and Uemura, which is still adopted today for its simplicity [2]. But a more complete and comprehensive theory is by T. Ando which is by far the best available model regarded by the researchers [3,4]. Ando treated various source terms contributing towards surface roughness in detail. Recently Jin and co-workers have extended Prang and Ando's model to SOI (silicon on insulator) structures where the severity of surface roughness has been predicted to hinder ballistic transport in ultra thin SOI MOSFETS [5].

This chapter is organised as follows: an introduction to the underlying physics of the problem and the statistical measure to compute the "surface randomness" is given. Next various scattering potentials associated with surface roughness are presented. Surface roughness limited mobilities are simulated, incorporating the source terms presented in the previous section and their relative strengths are also compared.

Remote surface roughness model presented by Gámiz et al. and appropriate modification to it is also discussed along with the explanation to the observed trend in remote SR limited mobility.

11.2 Physics of the Problem

Surface Roughness (SR) in the context of MOS structures is associated with random fluctuations of the boundary between the insulator and the substrate. This roughness appears as atomic "steps" at the interface between the two materials. Deviation from the ideal flat surface introduces electric potentials from number of sources e.g. dipoles created at the interface, associated image charges, etc.

Moreover, wavefunctions of charge carriers are also physically perturbed from their normal states and consequently the potential of the system changes as well (wavefunctions and electrostatic potential are linked together via Schrödinger-Poisson coupled equations). Thus, charge carriers interact with the rough surface via these potentials and their momentum dissipates in the process.

Surface topology is usually unknown, thus it has to be modeled appropriately. Quantitatively roughness is measured via a 2D roughness function, $\Delta(\mathbf{r})$, which describes the fluctuations from an assumed ideal flat boundary. The two- dimensional vector $\mathbf{r}$ is measured along the interface plane.

The autocovariance function $C(\mathbf{r})$ determines the statistical properties of the roughness function $\Delta(\mathbf{r})$, which depends on two parameters viz.: Δ – the rms height of the steps and Λ – the average width of the fluctuation (see Fig. 11.1 for illustration). Mathematically it is given by:

$$C(\mathbf{r}) = \left\langle \Delta(\mathbf{r})\, \Delta(\mathbf{r} - \mathbf{r}') \right\rangle \tag{11.1}$$

which simply gives the probability of a random step at position $\mathbf{r}$ to be repeated at $(\mathbf{r} - \mathbf{r}')$, the notation in (11.1) $\langle \bullet \rangle$ represents the average value of a function.

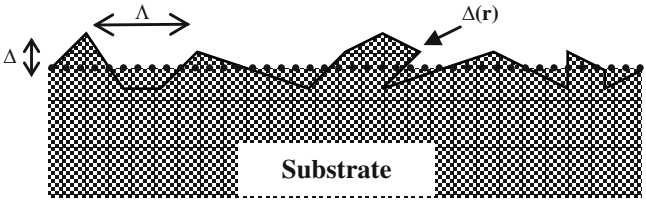

Fig. 11.1 Roughness function with the two parameters, Λ and Δ, illustrated

In relation to surface roughness, two forms of the autocovariance function are widely accepted – The Gaussian form, first proposed by Prang and Nee [1] and the exponential function [6]. Mathematically they are given as:

$$\begin{aligned} C(\mathbf{r}) = \left\langle \Delta(\mathbf{r})\, \Delta(\mathbf{r}-\mathbf{r}') \right\rangle &= \Delta^2 e^{-r^2/\Lambda^2} \qquad (\textit{Gaussian}) \\ &= \Delta^2 e^{-r/\Lambda} \qquad (\textit{Exponential}) \end{aligned} \tag{11.2}$$

Fourier transformation is needed to convert the autocovariance function from real space into **k**-space. Also according to Wiener–Khinchin theorem the Fourier transform of the autocovaraince function is in fact the "Power Spectrum Density", $|S(q)|^2$ of the function. Gaussian form mimics the nature ("Normal distribution") and has the other advantage that its Fourier transform is again Gaussian and thus easy to manipulate. However, Goodnick et al. [6] showed that the exponential form of the autocovariance fits more accurately to experimental data, measured through High Resolution Transmission Electron Microscope (HRTEM). The exponential form is expected for a stochastic Markov process [7]. The power spectrums for the two forms are given by [6]:

$$\begin{aligned} |S(q)|^2 &= \pi\Lambda^2\Delta^2 e^{(-q^2\Lambda^2/4)} \qquad (\textit{Gaussian}) \\ &= \pi\Lambda^2\Delta^2(1+q^2\Lambda^2/2)^{-\frac{3}{2}} \qquad (\textit{Exponential}) \end{aligned} \tag{11.3}$$

In simulations the exponential form will be utilized, which is, as stated, more consistent with measurement. Surface roughness limited mobility is greatly affected by the choice of Λ and Δ which are obviously device process dependent. In literature the range of these two parameters widely varies as: $\Lambda = 0.5 - 2.0\,\text{nm}$ and $\Delta = 0.2 - 0.7\,\text{nm}$ [7–10].

11.3 Associated Scattering Potentials

According to Ando's argument there are two main sources of surface roughness scattering affecting the charge carrier's motion, viz. [3, 4]:

- Fluctuation of *wavefunctions* due to physical "steps" at the interface ($\Gamma^{(1)}$)
- Fluctuation in *potential energy* due to Coulomb interactions

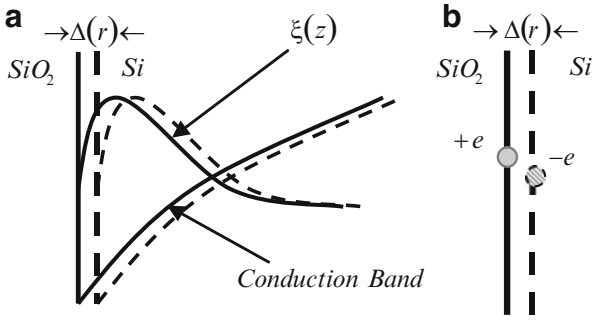

Fig. 11.2 *Solid lines* depicting the "normal" situation whereas *dashed lines* are presenting the distortions due to the interfacial "steps". (**a**) Wavefunctions and the conduction band edge are perturbed at the interface. (**b**) Image charge and a dipole are illustrated

The effects of "change in the potential energy" are further classified as

- Change in image potential ($\Gamma^{(2)}$)
- Creation of interface polarization charges ($\Gamma^{(3)}$)
- Fluctuation in charge carrier densities ($\Gamma^{(4)}$)

The first main source of scattering is obvious, since the "steps" at the interface perturbs the surface potential which consequently affects the wavefunctions, eigenvalues, etc. (see Fig. 11.2a), or simply the wavefunctions originate from the two surfaces: perturbed and unperturbed. This change in wavefunctions is propagated all along the depth of the substrate.

In order to compute the channel mobility the matrix element arising from the scattering potentials is required. Matrix element associated with change in wavefunctions is given by [5, 11]:

$$\Gamma_{i,j}^{(1)} = \int_0^\infty \left\{ \xi_i(z) \frac{\partial V(z)}{\partial z} \xi_j(z) + E_i \frac{\partial \xi_j(z)}{\partial z} \xi_i(z) + E_j \frac{\partial \xi_i(z)}{\partial z} \xi_j(z) \right\} dz \quad (11.4a)$$

where i and j stand for initial and final subbands of a conduction valley, respectively, E_i is the eigenvalue corresponding to the wavefunction ξ_i. The potential well in the substrate is denoted by V (in units of energy e.g. eV).

Next among the "Coulomb pieces" i.e. SR induced charge fluctuations: the scattering potential associated with the second term ($\Gamma^{(2)}$) appears due to the mismatch of the dielectric constants of the two materials (Si and SiO_2) across the interface. SR deforms the image potential developed at the surface. M. Saitoh studied 2D electrons on the surface of ^{4}He fluid and calculated the potential resulting from such image charges, this idea and expression was utilized in the context of 2DEG in inversion layer by Ando [4, 12].

Scattering matrix for the change in image potential is given by:

$$\Gamma^{(2)}_{i,j}(q) = \frac{e^2\tilde{\varepsilon}q^2}{16\pi\varepsilon_s}\int_0^\infty \xi_i(z)\left\{\frac{K_1(qz)}{qz} - \frac{\tilde{\varepsilon}}{2}K_0(qz\right\}\xi_j(z)\,dz \tag{11.4b}$$

where $\tilde{\varepsilon} = (\varepsilon_s - \varepsilon_{ox})/(\varepsilon_s + \varepsilon_{ox})$ with ε_s and ε_{ox} as the dielectric constants of the substrate and the oxide, respectively. K_0 *and* K_1 are modified Bessel functions of the second kind and of order zero and one, respectively.

The third Coulomb interaction ($\Gamma^{(3)}$) is also related to the difference in dielectric constants of the adjacent materials. An extra polarization charge is formed which changes the electric field distribution [13]. The arising electrostatic potential is calculated by considering an effective dipole moment at $z = 0$. The matrix element pertaining to $\Gamma^{(3)}$ is given by [5, 13]:

$$\Gamma^{(3)}_{i,j}(q) = e\tilde{\varepsilon}\int_0^\infty \xi_i(z)\left\{E_{\mathit{eff}}e^{-qz}\right\}\xi_j(z)\,dz \tag{11.4c}$$

where e is the electronic charge and E_{eff} is the effective field at the substrate side of the interface.

Lastly, the fluctuations at the interface also affect the electron distribution normal to the interface ($\Gamma^{(4)}$ term). The redistributed electron charges give rise to an additional scattering potential whose matrix element is [5, 14]:

$$\Gamma^{(4)}_{i,j}(q) = -\frac{e^2}{2q\varepsilon_s}\int_0^\infty \xi_i(z)\xi_j(z)dz\int_0^\infty \left\{e^{-q|z-z'|} + \tilde{\varepsilon}e^{-q|z+z'|}\right\}\frac{\partial n(z')}{\partial z'}dz' \tag{11.4d}$$

where $n(z)$ is the volume density of electrons along the z-direction (normal to the interface).

All the three "Columbic potentials" are wave vector $q = \left|\mathbf{k}_j - \mathbf{k}_i\right|$ dependent while potential due to change in wavefunctions is only electron energy dependent. It is to be noted that matrix elements given above are under the assumption of infinite potential barrier at the interface and vanishing wavefunctions deep into the thick substrate.

With four different source terms contributing in SR scattering, an "effective" matrix element is required whose squared value could be plugged in the scattering rate computed through Fermi golden rule [11].

It is well known that the scattering potential is effectively "screened" by the sheet of electrons present between the source of the electric potential and the scattered charge carriers, within certain specific distance called as the Debye length [7, 13]. Screening has a profound effect on the SR limited mobility; it is thus inevitable to include screening effects in simulations. SR limited mobilities are calculated using appropriate expressions in this context [14].

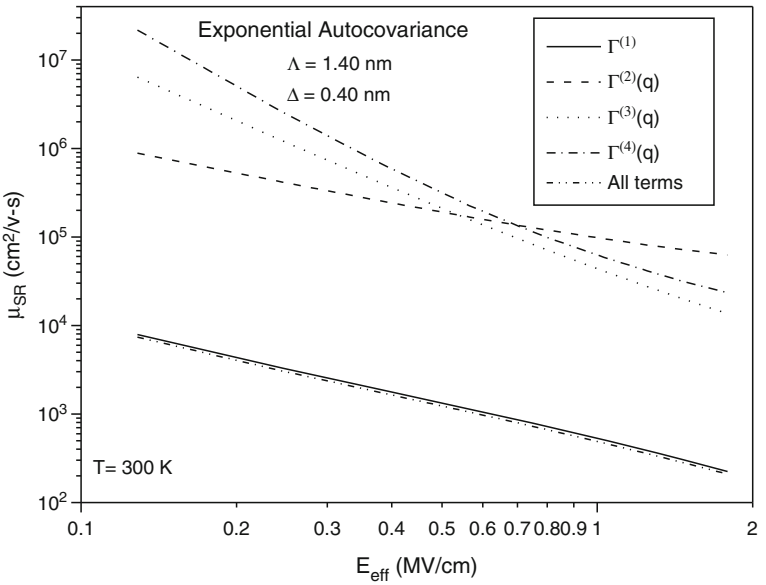

Fig. 11.3 Relative strengths of four sources of SR scattering are compared. The most damaging source for channel mobility is the $\Gamma^{(1)}_{i,j}$ term

11.4 Relative Strength of the Scattering Potentials

Once the screening mechanism is formulated the SR limited mobilities can be evaluated using the above mentioned four scattering potentials. Next, the relative importance of each scattering potential is evaluated. Figure 11.3 is a compilation of the results for SR mobility with the effects of individual scattering terms and with their combined influence.

It is clearly evident that the most dominant scattering source is due to the perturbations in electron wavefunctions ($\Gamma^{(1)}$). The weakest source is the variation of electron density due to physical "steps" introduced i.e., $\Gamma^{(4)}(q)$, though computationally it is a most time consuming term to evaluate. The percentage difference between mobility computed with all terms and then with $\Gamma^{(1)} + \Gamma^{(2)}(q) + \Gamma^{(3)}(q)$ terms is around 1% at $E_{eff} = 1\,\mathrm{MV/cm}$. Thus these three terms are sufficient to account for SR scattering and $\Gamma^{(4)}(q)$ can be safely ignored.

11.5 Remote Surface Roughness Scattering

Another scattering mechanism, closely related to SR scattering, is the "Remote Surface Roughness" (RSR) scattering. For ultra thin oxide layered MOS structures, charge carriers in the channel can significantly dissipate their momentum

by remotely interacting with the gate/insulator interface. Similar to oxide/substrate interface the second interface i.e. gate/oxide interface is not smooth and deviates from the ideal plane. Degree of roughness at the two interfaces is uncorrelated and depends on the device processing mechanism.

Extending the concept first presented by Li [15], Gámiz et al. proposed a simple scattering model for the remote surface roughness mechanism [16, 17]. In their proposed model the Hamiltonian of the system is given by:

$$H' = H_0 + \frac{\Delta V(z)}{\Delta_m}\Delta(\mathbf{r}) \tag{11.5}$$

where:

$$\Delta V(z) = V_{t_{ox}+\Delta_m}(z) - V_0(z) \tag{11.6}$$

with $V_{t_{ox}+\Delta_m}$ as the perturbed potential in the presence of "steps" at the gate/insulator interface while V_0 is the unperturbed potential i.e. in the case of ideal boundary. Surface topology is measured via 2D roughness function, $\Delta(\mathbf{r})$, which describes the fluctuations from an assumed ideal flat boundary. The two-dimensional vector $\mathbf{r}$ is measured along the interface plane. H_0 is the initial unperturbed Hamiltonian and the final Hamiltonian H' arising from the change in potential energy along the z-direction. The rms value of the step height at the second interface is denoted by Δ_m. Using the Hamiltonian (11.5) the matrix element was constructed as [16]:

$$\Gamma_{i,j}^{RSR} = \int_0^\infty \xi_i(z)\frac{\Delta V(z)}{\Delta_m}\xi_j(z)dz \tag{11.7}$$

The matrix element (11.7) modulated by dielectric function $\varepsilon(q)$ is utilized to compute the RSR scattering rate. However, Hamiltonian (11.5) of the present system can also be used to construct a relatively better RSR matrix element, following the approach described below:

Consider the change in the Hamiltonian of the system due to the presence of a random "step" at the interface, given by:

$$\Delta H = H' - H_0 \tag{11.8}$$

Next the matrix element for the changed Hamiltonian is generated from Eq. (11.8):

$$\Gamma_{i,j}^{0}(\mathbf{r}) = \int_0^\infty \xi_i(z + \Delta(\mathbf{r}))[H']\xi_j(z + \Delta(\mathbf{r}))dz - \int_0^\infty \xi_i(z)[H_0]\xi_j(z)dz \tag{11.9}$$

Note that for the final Hamiltonian H', the final perturbed wavefunctions are used. This perturbation is caused due to the potential difference arising at the gate/oxide interface. Substituting Eq. (11.5) in (11.9) to get:

$$\Gamma^0_{i,j}(\mathbf{r}) = \int_0^\infty \xi_i(z+\Delta(\mathbf{r}))\left[H_0 + \frac{\Delta V(z)}{\Delta_m}\Delta(\mathbf{r})\right]\xi_j(z+\Delta(\mathbf{r}))dz - \int_0^\infty \xi_i(z)[H_0]\xi_j(z)\,dz \tag{11.10}$$

Next using Taylor's theorem for the expansion of the wavefunctions to the lowest order reveals:

$$\Gamma^0_{i,j}(\mathbf{r}) = \int_0^\infty \left[\xi_i(z) + \frac{\partial\xi_i(z)}{\partial z}\Delta(\mathbf{r})\right]\left[H_0 + \frac{\Delta V(z)}{\Delta_m}\Delta(\mathbf{r})\right] \left[\xi_j(z) + \frac{\partial\xi_j(z)}{\partial z}\Delta(\mathbf{r})\right]dz - \int_0^\infty \xi_i(z)\,[H_0]\,\xi_j(z)\,dz \tag{11.11}$$

Ignoring the product terms involving $\Delta(\mathbf{r})^2$:

$$\Gamma^0_{i,j}(\mathbf{r}) = \int_0^\infty \left[\begin{array}{l} \xi_i(z)H_0\xi_j(z) + H_0\xi_i(z)\dfrac{\partial\xi_j(z)}{\partial z}\Delta(\mathbf{r}) + \\ \\ \xi_i(z)\,\dfrac{\Delta V(z)}{\Delta_m}\Delta(\mathbf{r})\,\xi_j(z) + H_0\xi_j(z)\dfrac{\partial\xi_i(z)}{\partial z}\Delta(\mathbf{r}) \end{array}\right]dz - \int_0^\infty \xi_i(z)\,[H_0]\,\xi_j(z)\,dz \tag{11.12}$$

Now, from the time independent Schrödinger equation:

$$H_0\xi = E\xi \tag{11.13}$$

Equation (11.12) is modified using (11.13) and after simplification the net result is:

$$\Gamma^0_{i,j}(\mathbf{r}) = \Delta(\mathbf{r})\int_0^\infty dz\left[\begin{array}{c} \xi_i(z)\dfrac{\Delta V(z)}{\Delta_m}\xi_j(z) + E_j\dfrac{\partial\xi_i(z)}{\partial z}\xi_j(z) \\ \\ +E_i\dfrac{\partial\xi_j(z)}{\partial z}\xi_i(z) \end{array}\right] \tag{11.14}$$

$$\Gamma^0_{i,j}(\mathbf{r}) = \Delta(\mathbf{r})\,\Gamma^{RSR}_{i,j} \tag{11.15}$$

where,

$$\Gamma_{i,j}^{RSR} = \int_0^\infty dz \left[\begin{array}{c} \xi_i(z)\dfrac{\Delta V(z)}{\Delta_m}\xi_j(z) + E_j\dfrac{\partial \xi_i(z)}{\partial z}\xi_j(z) \\ +E_i\dfrac{\partial \xi_j(z)}{\partial z}\xi_i(z) \end{array} \right] \tag{11.16}$$

is the modified form of the matrix element given earlier in Eq. (11.7).

In (11.16) the derivative of the electron wavefunctions appears, which essentially is a characteristic of surface roughness scattering [1]. The matrix element given in (11.6) over estimates the RSR limited mobility as compared to one in computed using (11.14). Another shortcoming of the Gámiz model is that the effect of rms Δ_m is not present explicitly (it cancels out in the scattering rate when squared matrix element is multiplied with power spectrum $|S(q)|^2$). The only weak dependence of Δ_m appears in Gámiz model is through simulated value of $\Delta V(z)$ (via the coupled Schrödinger Poisson solver) in (11.6), while the modification presented here to the transport model includes Δ_m explicitly and thus its effect is realistically observed.

For comparison, results obtained using the two model equations are shown in Fig. 11.4. In this study, two different theoretical values of Δ_m (0.5 and 0.3 nm) are used for a fixed oxide thickness of 1.0 nm. Potential $\Delta V(z)$ in (11.6) with wavefunctions and eigenvalues are computed using UT-Quant Schrödinger-Poisson solver [18]. With $\Delta_m = 0.5$ nm, the drop from the "Universal mobility" is around 5% at $E_{\text{eff}} \sim 1\text{MV/cm}$.

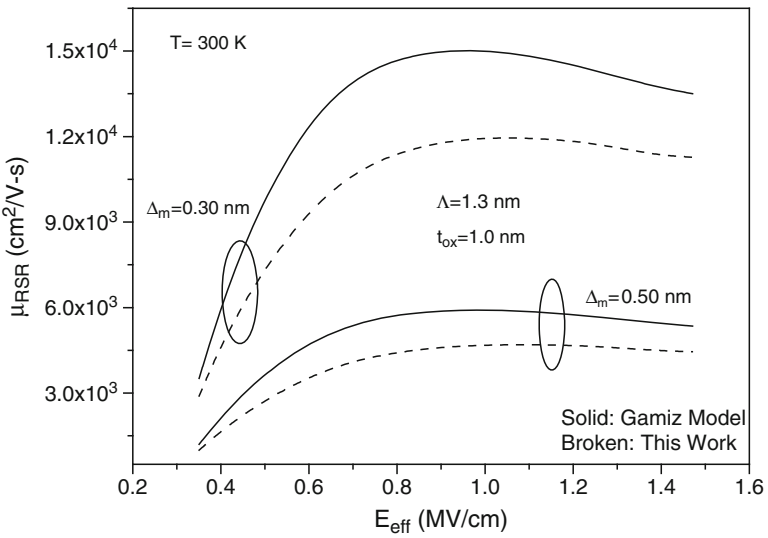

Fig. 11.4 RSR limited mobility computed using Gámiz et al. model [16] and the modified model proposed in this work. Gámiz model overestimates the mobility as compared to the modified model

11.5.1 Observed Trend in RSR Mobility

From Fig. 11.4 two observations can be clearly made, first: smoother the surface (small Δ_m) better is the RSR limited mobility. The reason for this behavior is obvious. Secondly: Initially RSR mobility increases with increasing sheet density, N_s, after reaching to an absolute maximum, mobility then starts declining. Possible reasons for this trend are explored below.

The scattering potential, which is in fact the difference in perturbed and unperturbed potentials ($V_{t_{ox}+\Delta_m}(z) - V_0(z)$), decreases with evolving sheet density, N_s. Figure 11.5 illustrates this fact graphically. Additionally, screening also contributes towards mobility enhancement. On the other hand, with increasing transverse field, the wavefunctions are more squeezed towards the interface and thus magnitude of the matrix element increases, consequently lowering the mobilities (see (11.7) or (11.16)). At the maximum ("breakeven point"), observed in Fig. 11.4, the two effects i.e. $\Delta V(z)$ and the "squeezing wavefunctions" just balance each other. Beyond this point, a further increase in gate voltage favors the impact of squeezed wavefunctions and thus mobility starts dropping, similar to the trend observed in "normal" SR mobility.

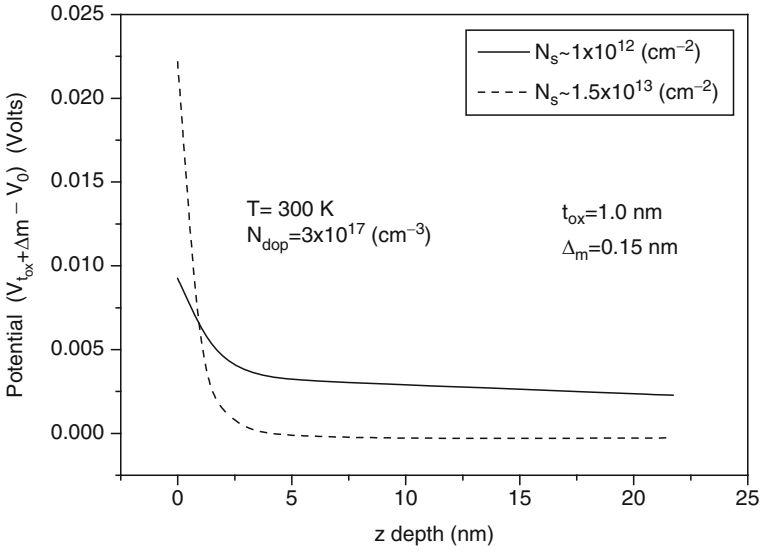

Fig. 11.5 Difference in the unperturbed and perturbed potentials are plotted for two different sheet concentrations. For strong inversion the difference in potentials ΔV drops sharply

References

1. Prange, R.E., Nee, T.W.: Quantum spectroscopy of the low-field oscillations in the surface impedance. Phys. Rev. **168**, 779–786 (1968)
2. Matsumoto, Y., Uemura, Y.: Scattering mechanism and low temperature mobility of MOS inversion layers. Jpn. J. Appl. Phys. (suppl.2, pt.2), 367–370. Kyoto, Japan (1974)
3. Ando, T.: Screening effect and quantum transport in a silicon inversion layer in strong magnetic fields. J. Phys. Soc. Jpn. **43**, 1616–1626 (1977)
4. Ando, T., Fowler, A.B., Stern, F.: Electronic properties of two-dimensional systems. Rev. Mod. Phys. **54**, 437–672 (1982)
5. Seonghoon, J., Fischetti, M.V., Ting-Wei, T.: Modeling of surface-roughness scattering in ultrathin-body SOI MOSFETs. IEEE Trans. Electron Device **54**, 2191–2203 (2007)
6. Goodnick, S.M., Ferry, D.K., Wilmsen, C.W., Liliental, Z., Fathy, D., Krivanek, O.L.: Surface roughness at the Si(100)-SiO_2 interface. Phys. Rev. B **32**, 8171 (1985)
7. Ferry, D.K., Goodnick, S.M.: Transport in Nanostructures. Cambridge University Press, Cambridge (1999)
8. Jungemann, C., Emunds, A., Engl, W.L.: Simulation of linear and nonlinear electron transport in homogeneous silicon inversion layers. Solid-St. Electron. **36**, 1529–1540 (1993)
9. Pirovano, A., Lacaita, A.L., Zandler, G., Oberhuber, R.A.O.R.: Explaining the dependences of the hole and electron mobilities in Si inversion layers. IEEE Trans. Electron Devices **47**, 718–724 (2000)
10. Low, T., Li, M.F., Fan, W.J., Ng, S.T., Yeo, Y.C., Zhu, C., Chin, A., Chan, L., Kwong, D.L.: Impact of surface roughness on silicon and Germanium ultra-thin-body MOSFETs. IEEE international electron devices meeting 2004 (IEDM), pp. 151–154, 13–15 Dec 2004. San Francisco, CA.
11. Esseni, D.: On the modeling of surface roughness limited mobility in SOI MOSFETs and its correlation to the transistor effective field. IEEE Trans. Electron Devices **51**, 394–401 (2004)
12. Saitoh, M.: Warm electrons on the liquid ^{4}He surface. J. Phys. Soc. Jpn. **42**, 201–209 (1977)
13. Fischetti, M.V., Laux, S.E.: Monte-Carlo study of electron-transport in silicon inversion-layers. Phys. Rev. B **48**, 2244–2274 (1993)
14. Esseni, D., Abramo, A.: Modeling of electron mobility degradation by remote Coulomb scattering in ultrathin oxide MOSFETs. IEEE Trans. Electron Devices **50**, 1665–1674 (2003)
15. Jia, L., Ma, T.P.: Scattering of silicon inversion layer electrons by metal-oxide interface roughness. J. Appl. Phys. **62**, 4212–4215, Nov 15 1987
16. Gámiz, F., Roldan, J.B.: Scattering of electrons in silicon inversion layers by remote surface roughness. J. Appl. Phys. **94**, 392–399 (2003)
17. Gámiz, F., Godoy, A., Jimenez-Molinos, F., Cartujo-Cassinello, P.A.C.-C.P., Roldan, J.B.A.R.J.B.: Remote surface roughness scattering in ultrathin-oxide MOSFETs. 33rd Conference on European Solid-State Device Research, 2003 (ESSDERC '03), pp. 403–406 (2003)
18. Shih, S.J.W.-K., Chindalore, G.: UTQUANT 2.0 User's Guide. University of Texas Press, Austin (1997)